On-line control of the nonlinear dynamics for synchrotrons

J. Bengtsson
Brookhaven National Laboratories, Upton, New York 11973, USA

I. P. S. Martin and J. H. Rowland
Diamond Light Source, Oxfordshire OX11 0DE, United Kingdom

R. Bartolini*
Diamond Light Source, Oxfordshire OX11 0DE, United Kingdom and John Adams Institute, University of Oxford, Oxford OX1 3RH, United Kingdom

(Received 19 February 2015; published 6 July 2015)

We propose a simple approach to the on-line control of the nonlinear dynamics in storage rings, based on compensation of the nonlinear resonance driving terms using beam losses as the main indicator of the strength of a resonance. The correction scheme is built on the analysis of the resonance driving terms in first perturbative order and on the possibility of using independent power supplies in the sextupole magnets, which is nowadays present in many synchrotron light sources. Such freedom allows the definition of "smart sextupole knobs" attacking each resonance separately. The compensation scheme has been tested at the Diamond light source and proved to be effective in opening up the betatron tune space, resonance free, available to the electron beam and to improve the beam lifetime.

DOI: 10.1103/PhysRevSTAB.18.074002 PACS numbers: 41.85.-p, 05.45.-a

I. INTRODUCTION

The control of the nonlinear dynamics for circular accelerators dates back to the first synchrotrons [1]. Long term stability issues in colliders, and dynamics and momentum aperture enhancement in synchrotron light sources, have stimulated the development of a wealth of techniques to analyze and correct the nonlinear dynamics in storage rings [2–8].

Alongside this, the progress of high level instrumentation, such as high resolution turn-by-turn beam position monitors (BPMs) and single-turn kickers, has allowed significant steps forward to be made in the experimental characterization of the nonlinear beam dynamics [5–15]. However the on-line correction of nonlinear resonance remains a delicate exercise and alternative, possibly simpler strategies are still sought for and constitute an active research topic, both theoretically and experimentally.

In this paper we present the proof of principle of a new method for the on-line control of resonance driving terms based on the construction of a response matrix relating the driving terms with the sextupole families in the ring. This approach is underpinned by the identification of "smart sextupole knobs," i.e., combinations of sextupoles which effectively attack only a single given resonance driving term. Issues related to the degeneracy of the matrix are solved by introducing new sextupole families which remove the degeneracy. The correction of the individual driving terms is then uniquely based on the model response matrix and on the measurement of beam losses as the resonance is approached in the betatron tune space. The Diamond storage ring is an ideal test bed for such a technique since it is equipped with a highly performing system of diagnostics and instrumentation. In particular, the method proposed takes full profit of the independent power supplies for each sextupole, which allows for maximal freedom in the definition of the sextupole families.

A prerequisite for systematic beam studies of the nonlinear dynamics is that the linear optics have been understood. In particular, the beta-beating and phase advance beat, the (local) linear coupling have been corrected to satisfactory levels, and the linear optics model has been calibrated. In fact, such corrections have become routine operation for synchrotron light sources thanks to Safranek's and Portmann's interactive linear optics from closed orbits (LOCO) tool [16].

The paper is organized as follows. The theory of the resonance driving terms and the details of the correction method proposed are reviewed in Sec. II. In Sec. III we describe the basic properties of the Diamond storage ring. In Sec. IV we present the results of a campaign of experimental tests in which this technique was applied to the Diamond storage ring lattice. The results show that the technique was capable of improving the beam lifetime by 10% over its initial value. This result is in line with

*Corresponding author.
riccardo.bartolini@diamond.ac.uk

previous investigations over the same lattice [6]. However, it accomplishes a much more straightforward correction as it is entirely based on a response matrix computed from the model and on the measurement of beam losses. The correction is fast and robust, does not require lengthy optimization computer runs and can be used as an on-line tool in the control room. Conclusions are drawn in Sec. V.

II. THEORETICAL BACKGROUND

In order to explain the correction method and to introduce the nomenclature, we briefly review the resonance driving terms theory. We then give the detailed strategy devised for the on-line control of the nonlinear beam dynamics referring in particular to resonances excited by sextupole.

A. The resonance driving terms

The resonance driving terms can be introduced within different equivalent theoretical frameworks: we use the Lie series formalism to write the Poincaré map $\mathscr{M}$ of the accelerator as a formal Lie series

$$\mathscr{M} = \mathcal{A}^{-1} e^{\mathcal{L}_{h(\bar{\phi},\bar{J})}} \mathcal{R}\mathcal{A},$$

where $[\bar{\phi},\bar{J}] \equiv [\phi^x, \phi^y, J_x, J_y]$ are the action-angle variables for the linear transverse dynamics, $\mathcal{A}$ a linear transformation to Floquet space [17], and $\mathcal{R} = \exp(\mathcal{L}_{-2\pi\bar{\nu}\cdot\bar{J}})$ a phase-space rotation. The Lie derivative $\mathscr{L}_{h(\bar{\phi},\bar{J})}$ is the usual Poisson bracket defined in Hamiltonian dynamics

$$\mathcal{L}_{f(\bar{\phi},\bar{J})} g(\bar{\phi},\bar{J}) \equiv \sum_k [\partial_{\phi^k} f(\bar{\phi},\bar{J})\partial_{J_k} g(\bar{\phi},\bar{J}) - \partial_{J_k} f(\bar{\phi},\bar{J})\partial_{\phi^k} g(\bar{\phi},\bar{J})].$$

In the case of midplane symmetry, the matrix representation for $\mathcal{A}$ is

$$A = \begin{bmatrix} \sqrt{\beta_x} & 0 \\ -\frac{\alpha_x}{\sqrt{\beta_x}} & \frac{1}{\sqrt{\beta_x}} \end{bmatrix}, \qquad A^{-1} = \begin{bmatrix} \frac{1}{\sqrt{\beta_x}} & 0 \\ \frac{\alpha_x}{\sqrt{\beta_x}} & \sqrt{\beta_x} \end{bmatrix},$$

where β_x and α_x are the usual Twiss functions. Similar relations hold for the y plane. In the case of nonzero dispersion, there is also a δ-dependent translation of the fix point ($\bar{x} = [x, y, p_x, p_y]$)

$$\bar{x}_{\mathrm{cod}} \to \bar{x}_{\mathrm{cod}} + \bar{\eta}\delta,$$

where $\bar{\eta}$ is the dispersion. Notice that we have considered here the evolution of the particle coordinates in the 4D transverse phase space, using the energy deviation $\delta = (E - E_0)/E_0$ as an adiabatic parameter. The formalism can be easily extended to the full 6D case.

The generator $h(\bar{\phi},\bar{J})$ is given by

$$h(\bar{\phi},\bar{J}) = -\frac{q}{p_0}\int_0^C \mathcal{A}(s) A_s(\tilde{x},\tilde{y};s)ds,$$

where $A_s(x, y, s)$ is the longitudinal component of the vector potential, q the charge of the particle, p_0 the momentum of a reference particle, C the circumference, and $[\tilde{x},\tilde{y}]$ the linear solution in Floquet space

$$\tilde{x} = \sqrt{2J_x}\cos(\phi_x) = \sqrt{\frac{J_x}{2}}(e^{i\phi_x} + e^{-i\phi_x})$$

and similarly for y. The generator $h(\bar{\phi},\bar{J})$ has the form

$$h(\bar{\phi},\bar{J}) = \sum_{\bar{l}} h_{\bar{l}} J_x{}^{(i_1+i_2)/2} J_y{}^{(i_3+i_4)/2} \delta^{i_5} e^{i[(i_1-i_2)\phi_x + (i_3-i_4)\phi_y]}$$
$$\bar{l} \equiv [i_1, i_2, i_3, i_4, i_5],$$
$$|\bar{l}| = i_1 + i_2 + \cdots + i_5$$

and the coefficients $h_{\bar{l}}$ are the resonant driving terms. By introducing the multipole expansion of the vector potential

$$\frac{q}{p_0}A_s(x,y,s) = -\mathrm{Re}\left\{\sum_{n=1}^{\infty}\frac{1}{n}[ia_n(s) + b_n(s)](x+iy)^n\right\},$$
$$A_x(s) = A_y(s) = 0,$$

we obtain for the driving terms

$$h_{\bar{l}} = \frac{1}{n2^n}\binom{n}{i_1+i_2}\int_0^C \begin{Bmatrix} b_n(s) \\ a_n(s) \end{Bmatrix} [2\beta_x(s)]^{m_x/2}[2\beta_y(s)]^{m_y/2}\eta_x^{i_5} e^{i[n_x\mu_x(s) + n_y\mu_y(s)]}ds$$

$$m_x = i_1 + i_2, \qquad m_y = i_3 + i_4, \qquad n_x = i_1 - i_2, \qquad n_y = i_3 - i_4, \qquad n = |\bar{l}| - i_5,$$

where μ_x and μ_y are the horizontal and vertical phase advances respectively. The resonance driving terms depend on the global properties of the lattice and appear in complex conjugate pairs

$$h_{i_1 i_2 i_3 i_4 i_5} = h^*_{i_2 i_1 i_4 i_3 i_5}.$$

To summarize, by introducing the Lie series representation of the Poincaré map for Hamiltonian flow in action-angle variables and using the multipole expansion to model the magnets, the Lie derivative can be expressed as a sum of driving terms. We observe that, although the driving terms are computed at a particular section along the ring, the resulting Poincaré map is used to describe the dynamics over many turns and its optimization will reflect the optimization of the global properties of the lattice. In the next section we will outline an effective approach to address the related control problem, by explicitly solving the "inverse problem" for the driving terms.

B. The sextupole response matrix

We now show how to build a strategy for the control of the driving terms excited by the sextupoles. The leading order driving terms from (normal) sextupoles

$$\frac{q}{p_0}A_s(s) = -b_3(s)\frac{1}{3}(x^3 + 3xy^2),$$

i.e., that are linear in the sextupole strengths b_3, are [18]

$$\bar{h} = [h_{11001}, h_{00111}, h_{21000}, h_{10110}, h_{30000}, h_{10200}, h_{10020}, h_{20001}, h_{00201}, h_{10002}].$$

The first two are real (driving linear chromaticity), but the other eight have both sine and cosine terms, so there is a total of 18 terms. The effects on the dynamics are summarized in Table I. The driving terms for the second order dispersion, h_{10002} is weak for the Diamond lattice so it was not included in the compensation procedure.

We introduce the sextupole response matrix (SRM) S by

$$\overline{\Delta h} = \frac{\partial \bar{h}}{\partial \overline{b_3}}\overline{\Delta b_3} \equiv S\overline{\Delta b_3},$$

i.e., the Jacobian of the system. The matrix S can be inverted e.g., by singular value decomposition (SVD) [19]

$$\overline{\Delta b_3} = S^{-1}\overline{\Delta h}.$$

Hence, if we (i) compute S from the (linear) optics model, (ii) compute the (pseudo)inverse S^{-1} by SVD, (iii) we can implement S^{-1} on-line as a set of "smart sextupole knobs," where the "smart sextupole knobs" will move the sextupole families in a combination that is responsible for the excitation, or the correction, of only a defined driving term, leaving the others untouched in first order. In this way we have an effective method to control the individual driving terms, without affecting the others.

C. Choice of the sextupole configuration

While the ideal lattice is mirror symmetric at the center of the straight sections, i.e., the sine terms of the driving terms are zero at these points, the symmetry is slightly broken for a real lattice due to engineering tolerances, e.g., mechanical alignment and random magnetic multipole errors. So, to control both the sine and cosine terms, the mirror symmetry of the original eight sextupole families must be broken. A trivial choice is to e.g., split the lattice/sextupole families into a left half and a right half, therefore doubling the number of families to 16. However, this choice still maintained the sixfold symmetry of the lattice and did not remove the degeneracy in the SRM: the singular values structure still prevented an effective decoupling of the correction. We eventually divided the six super periods of the lattice sextupole families into three sections for a total of 24 families to remove the SRM degeneracy.

III. DIAMOND LATTICE PROPERTIES

Diamond is a state of the art, medium energy synchrotron light source [20] in operation since January 2007 [21]. The natural horizontal emittance is 2.7 nm·rad, the energy 3 GeV, and the circumference 561.6 m. The lattice is based on a 24 cells double bend structure with sixfold periodicity and dispersion in the straights. The linear optics is shown in Fig. 1. The nominal working point and (linear) chromaticity are

$$\bar{\nu} = [27.205, 12.360], \qquad \bar{\xi}^{(1)} = [1.8, 1.8].$$

The sextupoles are combined function magnets that integrate the dipole correctors (to control the orbit) and skew quadrupoles (to control the linear coupling). While all the sextupole magnets have independent power supplies, they are typically powered as eight families, maintaining the sixfold symmetry of the linear lattice.

TABLE I. Effects on the dynamics due to the first order sextupolar driving terms.

Driving term	h_{11001}, h_{00111}	h_{21000}, h_{10110}	h_{30000}	h_{10200}	h_{10020}	h_{20001}, h_{00201}	h_{10002}
Effect	$\xi^{(1)}_{x,y}$	$\partial_{J_x}\beta_x$	$3\nu_x$	$\nu_x + 2\nu_y$	$\nu_x - 2\nu_y$	$\partial_\delta \beta_{x,y}$	$\partial_\delta x_{\mathrm{cod}}$

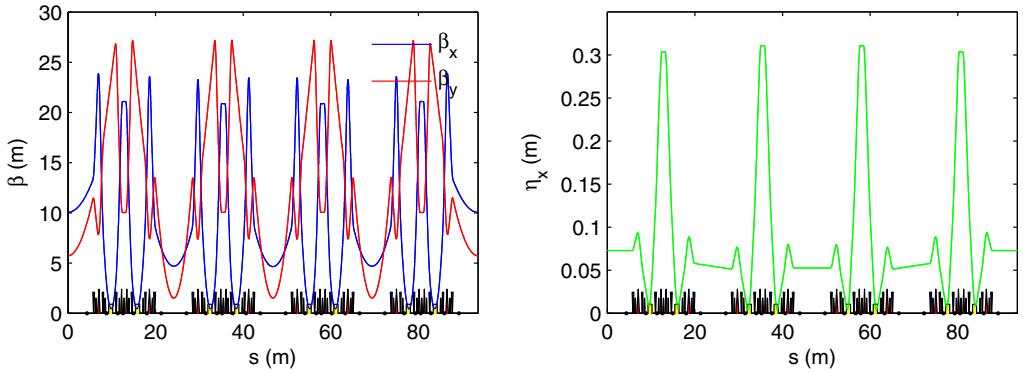

FIG. 1. Linear optics for Diamond in one super period: beta functions (left), dispersion (right).

The detuning with amplitude and the tune footprint are shown in Fig. 2 and the dynamic aperture (for the bare lattice) in Fig. 3.

The beam is injected at −8.3 mm from the injection orbit bump. However the bunch length from the Diamond booster is 26 mm and this lead to about (−3%, +2%) energy oscillation with −8.3 mm horizontal betatron oscillations. While neither the on- or off-momentum aperture is a concern (i.e., the injection efficiency is 80%–90% and the Touschek lifetime [22] is ∼25 hrs with 1% emittance coupling, with 0.3 mA per bunch), there remains potential for improvement with further suppression of the leading order sextupolar driving terms to make the injection process more robust. Diamond is therefore a perfect "test bench" for our method.

Being in operation since 2007, the linear optics of the machine is well understood and the experimental results obtained with the calibration of the linear model will not be reported here [23]. Figure 4 shows how the measured Touschek lifetime varies as a function of rf cavity voltage. Even though the lifetime is satisfactory, the maximum value is reached at about 2.5 MV showing that it is limited by the off-momentum dynamic aperture, rather than the rf bucket.

In fact, 4 MV of rf voltage is available and a naive estimate of the corresponding rf bucket height, reported in

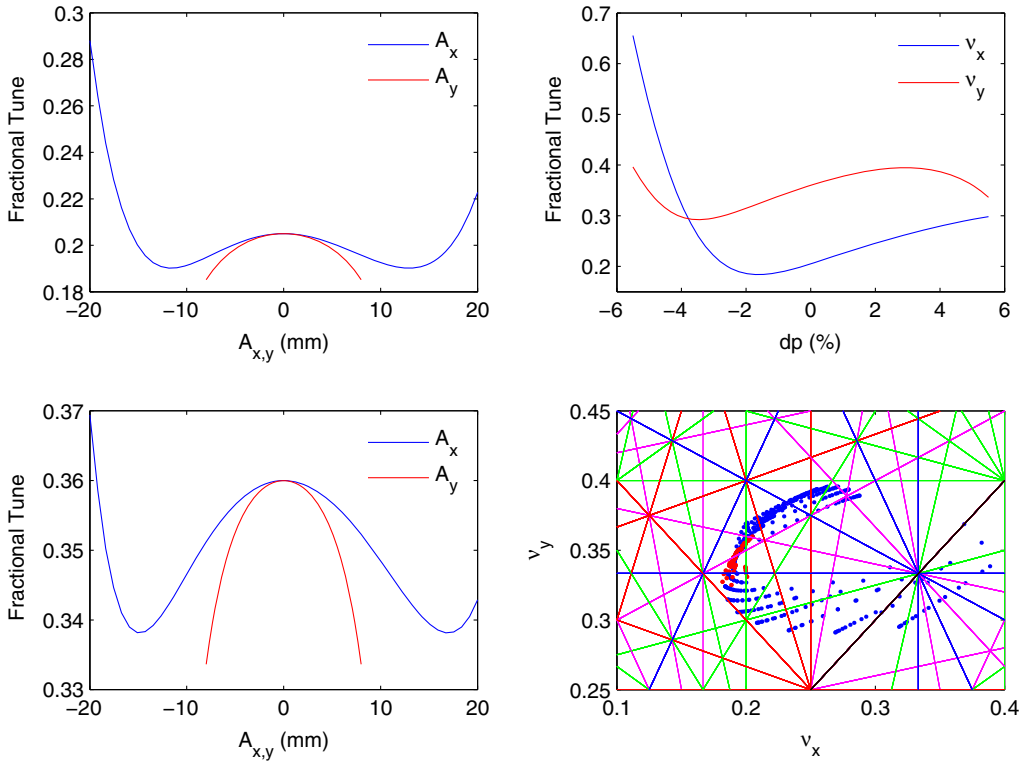

FIG. 2. Horizontal detuning with amplitude (top left), vertical (bottom left) and detuning with momentum (top right). Tune footprint for Diamond (bottom right) computed on the grid extending to $[\hat{x}, \hat{y}] = [15, 6.5]$ mm (in red) and $[\hat{x}, \hat{\delta}] = [10\text{ mm}, 4\%]$ (in blue).

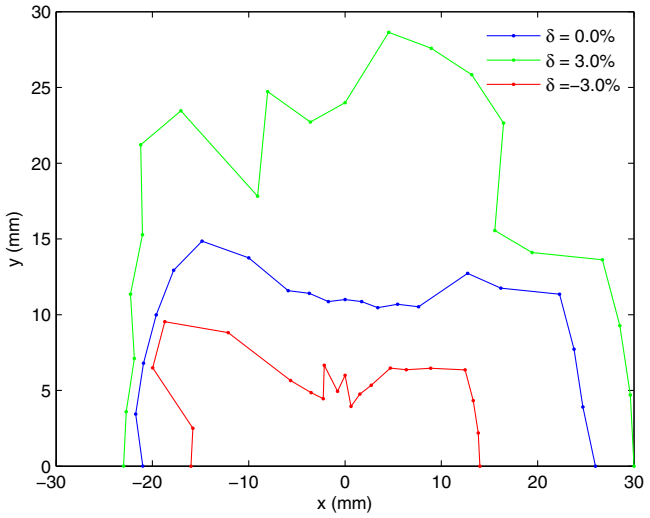

FIG. 3. Dynamic aperture for Diamond (bare lattice) at the injection point for different off-energy values.

Fig. 5, shows that the momentum aperture should extend to more than ±5%, were it is dependent only on the rf aperture. Given the tune footprint of Fig. 2, it is clear that to improve the momentum aperture substantially, the leading order sextupolar resonances must be crossed. In particular, $\nu_x + 2\nu_y = 52$ and $3\nu_x = 82$ are crossed for positive momentum deviation (1.5%) and negative momentum deviation (−4%) respectively. The remaining, i.e., $\nu_x - 2\nu_y = 3$, can be ignored since it is on the opposite side of the linear coupling resonance $\nu_x - \nu_y = 15$ which we assume cannot be crossed. On the other hand the resonance $3\nu_y = 37$ is also crossed at negative momentum deviation (−1.4%) and would require skew sextupole correctors knobs.

Further complications with the Diamond lattice appear due to a large second order momentum compaction factor.

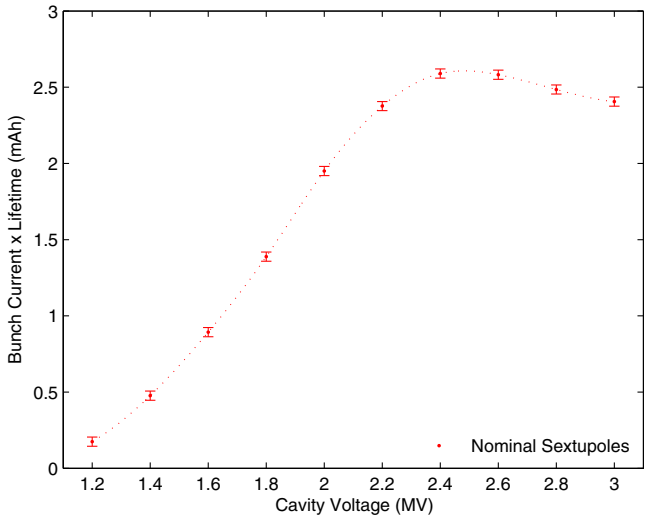

FIG. 4. Beam lifetime vs rf voltage for Diamond measured in single bunch for 0.15% coupling corrected with LOCO.

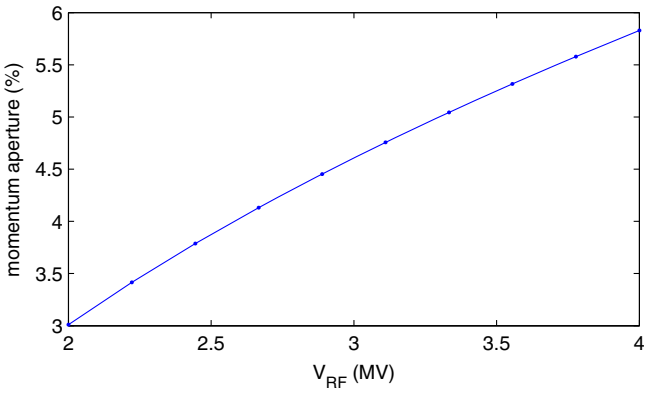

FIG. 5. Leading order estimate of momentum aperture vs rf voltage for Diamond.

The plot of the single particle trajectories in the longitudinal phase space reported in Fig. 6 shows clearly that the dynamics is quite distorted as compared to the traditional "rf bucket," due to nonlinear effects; also known as alpha buckets [24], and these effects have to be properly taken into account when assessing the available momentum aperture.

Indeed, it turns out that for high performance Double Bend lattices, i.e., with dispersion in the straights, $\alpha^{(1)}$ tends to become small, so the effect of $\alpha^{(2)}$ on the dynamics becomes significant. In particular, the Hamiltonian for the longitudinal motion to fifth order in the energy deviation is

$$H(\phi,\delta) = \frac{1}{2}h\alpha_c^{(1)}\delta^2 + \frac{1}{3}h\alpha_c^{(2)}\delta^3 + \frac{1}{4}h\alpha_c^{(3)}\delta^4 + \frac{qV_{\mathrm{RF}}}{2\pi E_0}[\cos(\phi+\phi_0) + \phi\sin(\phi_0)] + \mathcal{O}(\delta^5),$$

where $\phi_0 = -\mathrm{asin}(U_0/V_{rf})$, and the power series for the phase slip factor α_c defined as

$$\alpha_c \equiv \alpha_c^{(1)} + \alpha_c^{(2)}\delta + \alpha_c^{(3)}\delta^2 + \ldots.$$

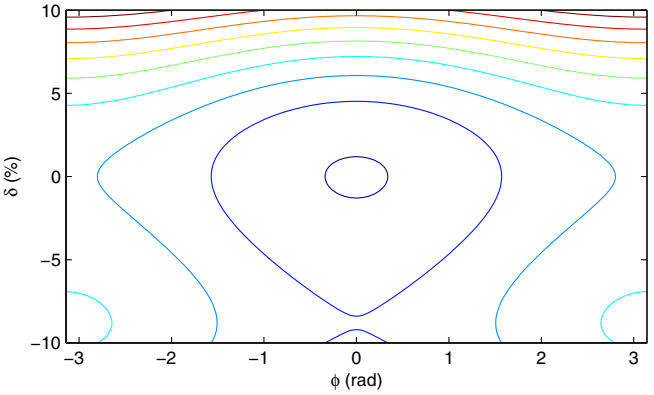

FIG. 6. Longitudinal phase space for Diamond with $V_{\mathrm{rf}} =$ 4 MV.

The equations of motion are

$$\delta' = -\partial_\phi H = \frac{qV_{\mathrm{RF}}}{2\pi E_0}[\sin(\phi+\phi_0)+\sin(\phi_0)] + \mathcal{O}(\delta^4)$$

$$\phi' = \partial_\delta H = h\alpha_c^{(1)}\delta + h\alpha_c^{(2)}\delta^2 + h\alpha_c^{(3)}\delta^3 + \mathcal{O}(\delta^4)$$

with the fix points

$$\delta_0 = 0, \qquad \delta_{1,2} = -\frac{\alpha_c^{(2)}}{2\alpha_c^{(3)}}\left(1 \pm \sqrt{1 - \frac{4\alpha_c^{(1)}\alpha_c^{(3)}}{(\alpha_c^{(2)})^2}}\right).$$

For Diamond we obtain a fixed point at $\delta_0 = 0$ and the next closest stable fixed point at $\delta_1 = -8.9\%$. In conclusion, it appears that currently the off-momentum aperture is limited to $\sim 3.5\%$ mainly due to the crossing of leading order sextupolar resonances in the betatron tune space. So, by correcting these resonances, in particular $\nu_x + 2\nu_y = 52$ and $3\nu_x = 82$, we expect to be able to improve the momentum aperture to $\sim 4.0\%$, limited by the alpha bucket, and correspondingly, increase the Touschek lifetime significantly.

IV. EXPERIMENTAL TECHNIQUE AND RESULTS

Driving terms can be analyzed with the measurement of the frequency content of the turn-by-turn data. However some care is required in order to extract significant information from next to leading spectral lines, often buried in the noise of the turn-by-turn data. The measurements are preferably done with a small linear chromaticity in order to reduce the decay of the signal due to phase space filamentation, possibly far from the operational condition of the machine. In order to obtain a reasonable signal, the working point must often be moved close to each individual resonance. Although the turn-by-turn beam quality can be improved, and indeed meaningful information on the

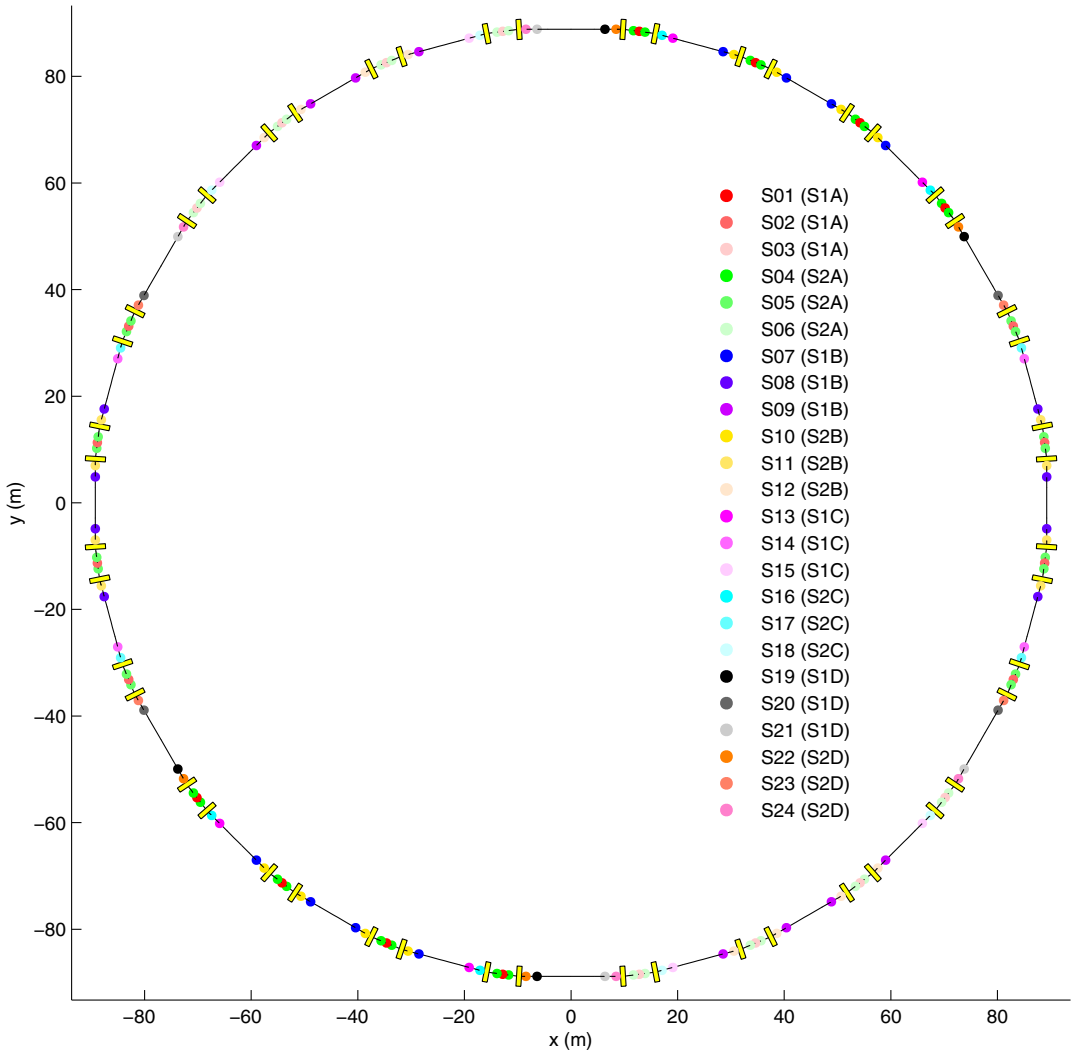

FIG. 7. Sextupole families for Diamond including the additional families introduced to generate "smart sextupole knobs" according to the on-line SRM technique. The old family split is indicated in the brackets.

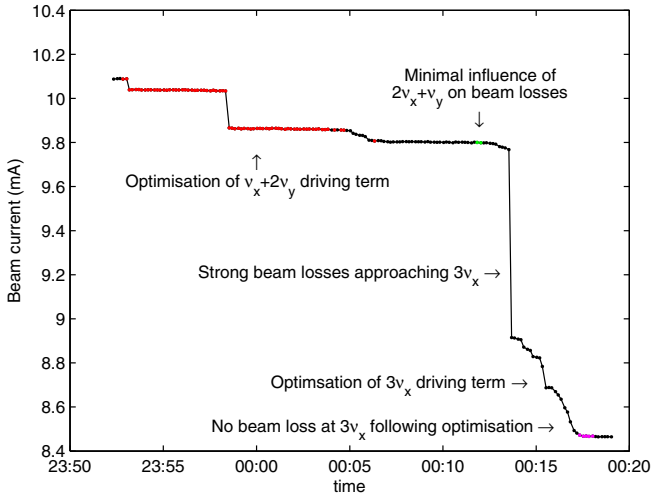

FIG. 8. Measured beam current during the sextupole optimization. See also Fig. 9 for further information.

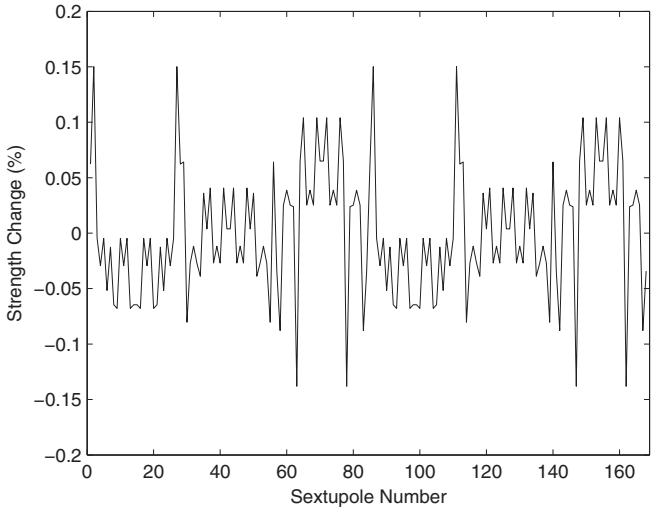

FIG. 10. Relative change in sextupole strengths as a result of the whole optimization.

driving terms can be extracted [6–8,11–15], we opted for the use of the observed beam loss on a beam current monitor as the main signal, indicating the strength of a resonance. We progressively moved the working point closer to the resonance, using quadrupoles, and adjusted the cosine- and sine terms of the corresponding resonant driving term with the inverted SRM tool and monitored the beam losses. As the betatron tunes get closer to the resonance, the initial beam losses were progressively decreased by adjusting the corresponding "smart sextupoles knob," until we are able to sit on the resonance without losses at all and with no perturbation on the stored beam. We found this approach to be much simpler, straightforward, robust and equally effective in improving the machine performance compared to the more delicate analysis of turn-by-turn data. The aforementioned splitting of the sextupoles in 24 families is illustrated in Fig. 7.

The procedure can tackle more than one resonance simultaneously. While the compensation of a particular resonance is straightforward, the associated (minor) change of linear optics brought about by shifting the working point using quadrupoles was enough to undo the compensation of a previous resonance when moving on to the next. We therefore introduced a suitable linear chromaticity and moved the working point by changing the energy, i.e., by adjusting the rf frequency, instead. By this approach, we could then compensate both $\nu_x + 2\nu_y = 52$ and $3\nu_x = 82$, without any beam loss, as shown in Figs. 8 and 9.

Having identified an effective procedure for applying the driving term corrections, further trials of the method were performed at the nominal user operating tune point and linear chromaticity. After again applying small corrections of less than 0.2% to the sextupole strengths using the

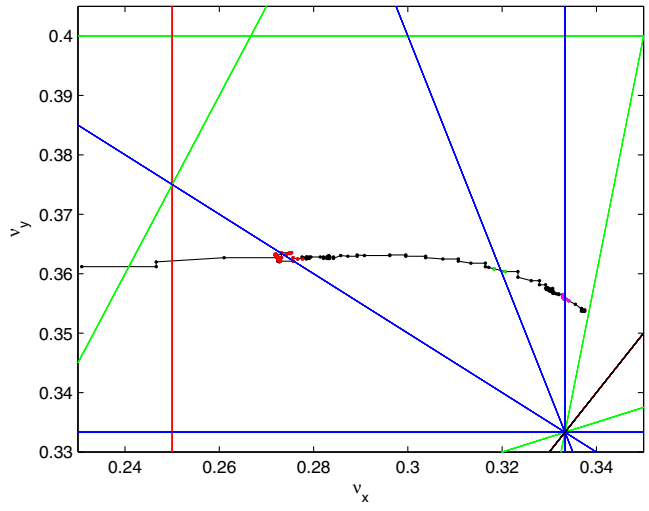

FIG. 9. Measured tune footprint during the sextupole optimization. The color code corresponds to the data of Fig. 8.

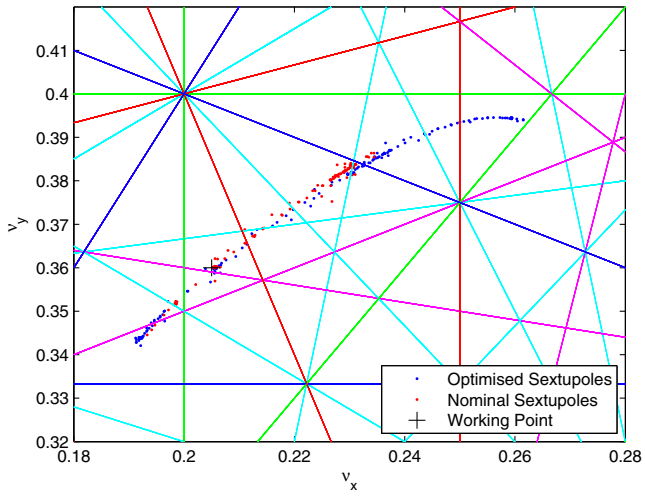

FIG. 11. Measured tune footprint before (red) and after (blue) the optimization of the sextupoles.

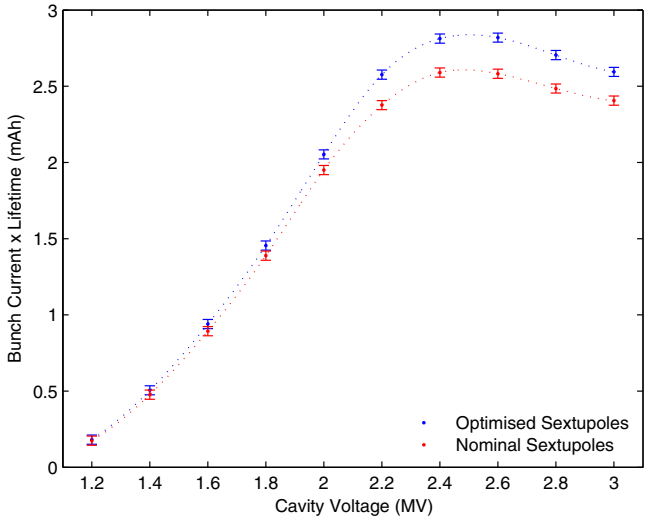

FIG. 12. Beam lifetime vs rf voltage after compensation of $\nu_x + 2\nu_y = 52$ and $3\nu_x = 82$. The red curve corresponds to the data before the optimization reported in Fig. 4.

inverted SRM tool (see Fig. 10), the $\nu_x + 2\nu_y = 52$ resonance could be compensated and beam losses previously observed when approaching this line could be completely eliminated. As anticipated, this led to a substantial increase in the off-momentum aperture available to the beam in the positive direction from $-1.0\%/+1.4\%$ to $-1.0\%/+2.8\%$ (see Fig. 11). As a result we increased the stable area available to the beam in the betatron tunes plane and eventually improved the Touschek lifetime. The resulting improvement in the beam lifetime is shown in Fig. 12 and amounts to a 10% increase at 2.5 MV. At present, further improvements to the beam lifetime are limited by the $3\nu_y = 37$ resonance, hit for negative momentum deviation at -1.4%. This resonance is driven by skew sextupole fields in first order, for which there is no effective handle in the Diamond lattice.

V. CONCLUSIONS

A technique for on-line control of the leading-order sextupole driving terms in the one-turn map has been described. By using the accelerator model, the response of each driving term to small changes in the sextupole strength can be determined, allowing a sextupole response matrix to be constructed. This can then be inverted and used for individual control of the driving term amplitudes through a suitable adjustment of sextupole strengths.

Experiments with this technique using the Diamond storage ring have demonstrated the effectiveness of the method, in particular by increasing the positive momentum aperture available to the beam and hence the beam lifetime. While it has been demonstrated that it is possible to compensate any particular resonance by moving the working point using a change to the quadrupole gradients, it was found that the resulting small changes to the linear optics undid the compensation of any previously optimized resonances.

The most robust method was found to be via shifting the working point close to the resonance of interest by a suitable change in the beam energy by altering the rf frequency and linear chromaticity.

In this case study we have focused on the effects of normal sextupoles to the first perturbative order. However, the method is not limited to this, i.e., it can easily be generalized to the control of resonances excited at higher perturbative order by sextupoles and also for arbitrary normal or skew multipole driving terms (assuming such trims are available). In fact, the method has the potential to provide a framework for complete, on-line control of the nonlinear beam dynamics.

ACKNOWLEDGMENTS

The work of J. B. is supported by the U.S. Department of Energy, Contract No. DE-SC0012704, the work of R. B. is supported by EuCARD-2 network cofunded by the partners and the European Commission under Capacities 7th Framework Programme, Grant Agreement No. 312453.

[1] A. Schoch, Theory of linear and non-linear perturbations of betatron oscillations in alternating-gradient synchrotrons, CERN Report No. 57–13, 1958.
[2] J. Bengtsson, Non-linear transverse dynamics for storage rings with applications to the Low-Energy Antiproton Ring (LEAR) at CERN, CERN Yellow Report No. 88–10, 1988.
[3] R. Bartolini and F. Schmidt, Normal form via tracking or beam data, *Part. Accel.* ***59****, 93 (1998)*.
[4] H. Dumas and J. Laskar, Global Dynamics and Long-time Stability in Hamiltonian Systems via Numerical Frequency Analysis, Phys. Rev. Lett. **70**, 2975 (1993).
[5] D. Robin, C. Steier, J. Laskar, and L. Nadolski, Global Dynamics of the Advanced Light Source Revealed through Experimental Frequency Map Analysis, Phys. Rev. Lett. **85**, 558 (2000).
[6] R. Bartolini, I. P. S. Martin, J. H. Rowland, P. Kuske, and F. Schmidt, Correction of multiple nonlinear resonances in storage rings, Phys. Rev. ST Accel. Beams **11**, 104002 (2008).
[7] G. Franchetti, A. Parfenova, and I. Hofmann, Measuring localized nonlinear components in a circular accelerator with a nonlinear tune response matrix, Phys. Rev. ST Accel. Beams **11**, 094001 (2008).
[8] R. Bartolini, I. P. S. Martin, G. Rehm, and F. Schmidt, Calibration of the nonlinear ring model at the Diamond light source, Phys. Rev. ST Accel. Beams **14**, 054003 (2011).
[9] C. Steier, D. Robin, L. Nadolski, W. Decking, Y. Wu, and J. Laskar, Measuring and optimizing the momentum aperture in a particle accelerator, Phys. Rev. E **65**, 056506 (2002).
[10] M. Hayes, F. Schmidt, and R. Tomas, Direct measurement of resonance driving terms at SPS at 26 GeV, in *Proceedings*

of the 8th European Particle Accelerator Conference, Paris, 2002 (EPS-IGA and CERN, Geneva, 2002), pp. 1290–1292.

[11] M. Benedikt, C. Carli, M. Chanel, F. Schmidt, and P. Urschütz, Betatron resonance studies at the CERN PS booster by harmonic analysis of turn-by-turn beam position data, in *Proceedings of the 9th European Particle Accelerator Conference, Lucerne, 2004* (EPS-AG, Lucerne, 2004), pp. 1915–1917.

[12] Y. Luo, M. Bai, R. Calaga, J. Bengtsson, W. Fischer, N. Malitsky, F. Pilat, and T. Satogata, Measurement and correction of third resonance driving term in the RHIC, in *Proceedings of the 22nd Particle Accelerator Conference, PAC-2007, Albuquerque, NM* (IEEE, New York, 2007), pp. 4351–4353.

[13] A. Streun, M. Böge, N. Abreu, M. Aiba, A. Lüdeke, Å. Andersson, and J. Bengtsson, Nonlinear beam dynamics studies at the SLS, in *Proceedings of the 2nd Workshop on Nonlinear Beam Dynamics in Storage Rings* (Diamond Light Source, UK, 2009).

[14] G. Vanbavinckhove, M. Aiba, A. Nadji, L. Nadolski, R. Tomas, and M.-A. Tordeux, Linear and nonlinear optics measurements at Soleil, in *Proceedings of the 23rd Particle Accelerator Conference, Vancouver, Canada, 2009* (IEEE, Piscataway, NJ, 2009), pp. 3877–3899.

[15] A. Franchi, L. Farvacque, F. Ewald, G. Le Bec, and K. B. Scheidt, First simultaneous measurement of sextupolar and octupolar resonance driving terms in a circular accelerator from turn-by-turn beam position monitor data, Phys. Rev. ST Accel. Beams **17**, 074001 (2014).

[16] G. Portmann and J. Safranek, MATLAB Based LOCO, in *Proceedings of the 8th European Particle Accelerator Conference, Paris, 2002* (Ref. [10]), pp. 1184–1186.

[17] G. Floquet, Sur les équations différentielles linéaires à coefficients périodiques, *Ann. École Norm. Sup.* ***12****, 47 (1883)*.

[18] J. Bengtsson, The SLS sextupole scheme: An analytic approach, SLS Note No. 9/97, 1997.

[19] W. H. Press, B. P. Flannery, S. A. Teukolsky, and W. T. Vetterling, *Numerical Recipes in C* (Cambridge University Press, Cambridge, 1992).

[20] Diamond Synchrootnr Light Source. Report of Design Specifications (The Green Book), Daresbury Laboratory (2002).

[21] R. Walker, Commissioning and status of the Diamond storage ring, in *Proceedings of the 4th Asian Particle Accelerator Conference, Indore, 2007* (RRCAT, Indore, India, 2007), pp. 66–70.

[22] C. Bernardini, G. F. Corazza, G. Di Giugno, G. Ghigo, J. Haissinski, P. Marin, R. Querzoli, and B. Touschek, Lifetime and Beam Size in a Storage Ring, Phys. Rev. Lett. **10**, 407 (1963).

[23] I. P. S. Martin, R. Bartolini, R. T. Fielder, E. C. Longhi, and B. Singh, Further advances in understanding and optimizing beam dynamics in the Diamond storage ring, in *Proceedings of the 11th European Particle Accelerator Conference, Genoa, 2008* (EPS-AG, Genoa, Italy, 2008), pp. 3032–3034.

[24] D. Robin, E. Forest, C. Pellegrini, and A. Amiry, Quasi-isochronous storage rings, Phys. Rev. E **48**, 2149 (1993).